Vol. 123 (2013) ACTA PHYSICA POLONICA A No. 1

Structural Properties and Temperature Behaviour of Optical Absorption Edge in Polycrystalline ZnO:X (Cu,Ag) Films

B. Kulyk[a,*], V. Figà[b], V. Kapustianyk[a], M. Panasyuk[a], R. Serkiz[a]
and P. Demchenko[c]

[a]Scientific-Technical and Educational Center of Low Temperature Studies, Scientific and Educational Center "FRACTAL", Department of Physics, Ivan Franko National University of Lviv
Dragomanova Str., 50, UA-79005 Lviv, Ukraine

[b]Department of Chemistry, University of Palermo, Viale delle Scienze — ed. 17, 90128 Palermo, Italy

[c]Department of Inorganic Chemistry, Ivan Franko National University of Lviv
Kyryla i Mefodiya Street, 6, UA-79005 Lviv, Ukraine

(Received April 30, 2012)

Silver- and copper-doped ZnO films were prepared by radio-frequency magnetron sputtering on glass substrates. The influence of dopants content on the structural, morphological properties as well as on evolution of the optical absorption edge was considered. It has been found that Ag- and Cu-doped ZnO films are characterized by wurtzite crystalline structure with the preferred direction of crystalline orientation (002). The sizes of grains within the films were found to be dependent on the type of dopant. The temperature evolution of the optical absorption edge is described by the modified Urbach rule that reflects polycrystalline nature of the material. The corresponding parameters concerning electron– (exciton–) phonon interaction, phonon energies and temperature changes of the band-gap were determined and analysed.

DOI: 10.12693/APhysPolA.123.92

PACS: 68.37.Ps, 78.40.Fy, 68.55.ag

1. Introduction

ZnO is a very interesting material for many different applications in both microelectronic and optoelectronic devices. It is a wide bandgap oxide semiconductor with a direct energy gap of about 3.37 eV and high exciton binding energy of 60 meV at room temperature. Though, ZnO absorbs (UV) radiation due to band-to-band transition, it can be used as transparent conductive oxide thin film, mainly for applications such as solar cells, liquid crystal displays and heat mirrors [1–3]. Furthermore, ZnO is used in semiconducting multilayers, in gas sensors and optical position sensors, UV light-emitters, surface acoustic wave devices, piezoelectric transducers [4, 5]. During the last years ZnO has emerged as one of the most promising materials due to its optical and electrical properties, high mechanical and chemical stability together with its abundance in nature and non-toxicity. In order to improve the properties of ZnO films, several techniques such as sputtering, thermal evaporation, metal-organic chemical vapour deposition, spray pyrolysis, pulsed laser and electrochemical depositions have been applied for their production. The radio-frequency (rf) magnetron sputtering technique is one of preferred among these techniques since it is versatile and permits to produce the high-quality films for different applications.

The structural, physical and electrical properties of ZnO films were governed by deposition parameters [6], post-treatment [7–9] and doping material [10–16], such as Al, Ga, Sc, Y, Mn, Cu, Ag, etc. In addition, it is known that the metals of group I (Ag,Cu) would be considered as the fast-diffusing impurities in the semiconductor compound [6]. The diffusion of copper or silver into ZnO can cause changes in the characteristics of its structure and, therefore, in the other physical properties.

The Ag and Cu dopants in ZnO may behave like many other monovalent dopant ions, which have the ability to occupy both the lattice and interstitial sites (i.e. amphoteric dopants), that would be expressed as [13]:

$$2\mathrm{Ag} \xrightarrow{\mathrm{ZnO}} \mathrm{Ag}_{\mathrm{Zn}} + \mathrm{Ag}_{\mathrm{i}}, \tag{1}$$

$$2\mathrm{Cu} \xrightarrow{\mathrm{ZnO}} \mathrm{Cu}_{\mathrm{Zn}} + \mathrm{Cu}_{\mathrm{i}}. \tag{2}$$

The Ag and Cu centres in ZnO can occur in the following different charge states: Ag^0, Ag^+, Ag^{2+} and Cu^0, Cu^+, Cu^{2+}, respectively. When Ag^+ or Cu^+ substitute Zn^{2+} they act as acceptor in ZnO matrix, while the interstitial Ag^{2+} or Cu^{2+} are donors. However, Ag^0 and Ag^{2+} or Cu^0 and Cu^{2+} ions can easily lose or gain electron resulting in the formation of Ag^+ or Cu^+ that implies appearance of more acceptor centres [12]. Beside these dopant centres the other defects such as Zn_{i}, V_{O}, O_{i}, V_{Zn} can be present. They occur even in undoped ZnO [7]. The Ag-, Cu-doped ZnO films taken in various concentrations were already studied by photosensitivity, luminescent properties, electrical stability and have been

---

*corresponding author; e-mail: `bohdan_kulyk@yahoo.com`

used for different applications. Copper-doped ZnO is a good candidate in *p*-type ZnO [17] and sensors [18] as well as silver-doped ZnO are used in varistors [19], photocatalyst [20], etc. However, there are not many reports concerning the study of temperature behaviour of the optical absorption edge of such films. In this paper, therefore, we investigate the effect of dopants on structural, morphological features and temperature evolution of absorption edge in ZnO thin films.

2. Experimental details

The ZnO:Ag and ZnO:Cu thin films were deposited on glass substrates by means of rf-magnetron sputtering system from the targets of pressed ZnO powder (99.99%) together with metallic Ag or oxide CuO (99.99%) in argon–oxygen atmosphere at the gas pressure of 10^{-3} Torr. The argon partial pressure P_{Ar} (Ar/(Ar+O_2)) was 80%. In order to minimize the thermal stresses the substrate temperature was fixed at 300 °C. The target-to-substrate distance was 60 mm and rf-power — 100 W.

The atomic amount of Ag and Cu dopants in ZnO films (taken from energy dispersive X-ray (EDX) analysis using a REMMA-102-02 scanning electron microscope, working at 20 kV dc acceleration voltages in vacuum) was 1.6%, 5.9% and 0.5%, 1.5%, 3.3%, 5.0%, respectively. The thickness of ZnO thin films was estimated by the deposition time and by Dektak surface stylus profiler (model: Veeco) and was found to be about 1200 nm.

The X-ray diffraction (XRD) measurements were carried out using STOE STADI P diffractometer with linear position sensitive detector in transmission Bragg–Brentano geometry (Cu K_{α_1} radiation at $\lambda = 1.5406$ Å, Ge(111) monochromator, detector scanning step: 0.480°2θ, accumulation time: 320 s, 2θ angle resolution: 0.015°, 2θ range: 23–115°). The atomic force microscopy (AFM) scans were performed in contact mode using a Solver P47-PRO scanning probe microscope (NT-MDT). Processing of images was done using the Image Analysis program (NT-MDT).

The temperature evolution of the optical absorption edge was measured using a setup based on SF-4A quartz monochromator in the range from 350 to 450 nm.

3. Results and discussion

3.1. XRD analysis

The XRD spectra of ZnO and ZnO:Ag thin films of wurtzite structure are shown in Fig. 1 (also Table I). As one can see, the doping of ZnO film by a few percents of silver does not affect the crystalline structure of the film considerably. From the XRD patterns and as it is evident from previous reports [7, 10, 12, 13, 21–23], the silver-doped ZnO films have preferred orientation in the (002) direction. Besides, the additional low-intensity peaks corresponding to (100) and (101) directions in ZnO are observed. In the XRD spectra of ZnO film with higher amount of Ag ions (5.9 at.%) at $2\theta = 38.12°$ there appears a peak corresponding to the phase of silver. The relative intensity of (002)-peak in respect to the intensity of (101)-peak was found to be higher than those for the film with a lower Ag concentration (1.6 at.%). Since Ag^+ ions have a larger radius (0.122 nm) than Zn^{2+} (0.074 nm) they either substitute ions of Zn^{2+} that leads to distortion of the unit cell or segregate at the grain boundaries of ZnO and hence induce considerable disorder and faster grow of ZnO grains [13, 23]. Ag^+ would preferentially choose to sit in the vicinity of grain boundaries due to its large ionic radius. Thus, it is suggested that increase of the silver amount in ZnO film leads to its segregation at the grain boundaries and simultaneously decrease of the amount of substituted Ag^+ ions. Under such circumstances the crystalline quality of ZnO film appeared to be higher.

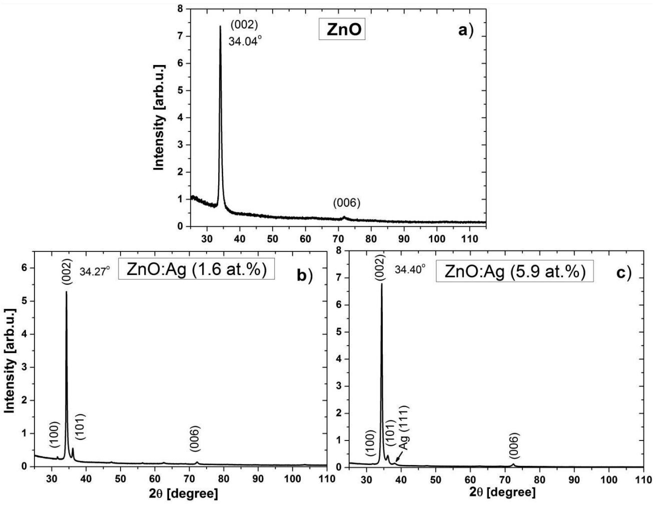

Fig. 1. XRD spectra of ZnO films: (a) ZnO undoped, (b) ZnO:Ag(1.6 at.%), (c) ZnO:Ag(5.9 at.%).

TABLE I

d-spacing of the (002) plane and FWHM of (002) peak of Ag and Cu-doped ZnO films taken from XRD spectra.

Film	*d* [Å]	FWHM [°]
ZnO	2.632	0.590
ZnO:Ag(1.6 at.%)	2.615	0.302
ZnO:Ag(5.9 at.%)	2.605	0.364
ZnO:Cu(0.5 at.%)	2.631	0.587
ZnO:Cu(1.5 at.%)	2.614	0.377
ZnO:Cu(3.3 at.%)	2.610	0.380
ZnO:Cu(5.0 at.%)	2.613	0.233

Figure 2 presents the XRD spectra of ZnO films doped by copper of various concentrations. It is important to note that ZnO:Cu films possess a more pronounced preferred direction of crystalline orientation (002) with the increase of atomic amount of Cu from 0.5 to 5.0%. This predicts that Cu ions occupy the lattice sites of ZnO [6, 8, 22, 24–26]. The radius of Cu^{2+} (0.072 nm) is a little smaller, meanwhile, the radius of Cu^{+} is larger than that of Zn^{2+} (0.074 nm). The substitution of Zn^{2+} ions is advantageous for Cu^{2+} because of their close radii. When Cu^{2+} ions substitute Zn^{2+} ions, the lattice constant decreases [25]. Besides, due to their small radius the copper ions can be interstitial dopants or would create the metallic clusters. The exception is ZnO:Cu(3.3 at.%) film in XRD spectra of which beside principal (002)-peak, a few other is noticeable including that one which corresponds to Zn phase. Such difference in structure of ZnO:Cu(3.3 at.%) film could be caused by the fluctuations during film deposition.

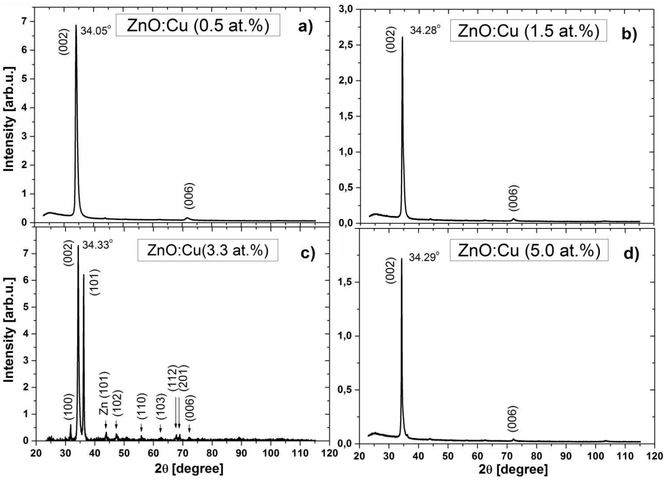

Fig. 2. XRD spectra of ZnO films: (a) ZnO:Cu(0.5 at.%), (b) ZnO:Cu(1.5 at.%), (c) ZnO:Cu(3.3 at.%), (d) ZnO:Cu(5.0 at.%).

Moreover, with the increase of copper or silver dopant amount, in the XRD spectra the shift of (002)-peak into direction of higher values of 2θ takes place in the XRD spectra due to isomorphous substitution of Zn^{2+} ions by Ag^{+} or Cu^{2+} ions. The parameters taken from these spectra are presented in Table I. With the increase of dopant (Ag,Cu) concentration the lattice d-spacing in doped ZnO films decreases. Meanwhile, the FWHM parameter for doped films is less than in undoped ZnO films.

3.2. Microstructure and morphology analysis

AFM micrograph analysis indicates the granular character of the deposited films. Figure 3 shows the AFM images of ZnO film and ZnO films doped with practically similar concentration of copper and silver dopant — 1.5 at.% and 1.6 at.%, respectively. The average grain size and the surface roughness obtained from those data (Table II) are connected with the amount of Cu or Ag dopants i.e. they decrease with increase of Cu concentration and increase with increase of Ag concentration. It is evident that the difference in the ionic radii of the dopants in respect of Zn^{2+} ion implies better ZnO grain growth during film deposition.

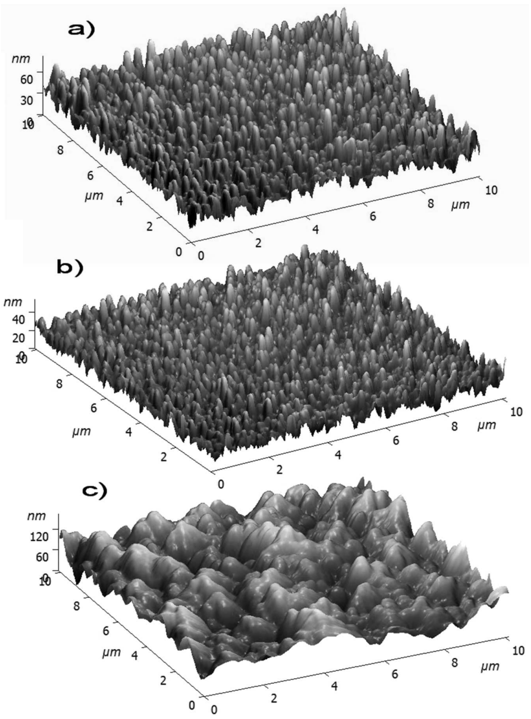

Fig. 3. AFM images of the films: (a) ZnO undoped; (b) ZnO:Cu(1.5 at.%); (c) ZnO:Ag(1.6 at.%).

TABLE II

Topological parameters of ZnO films,undoped and doped with Cu and Ag.

Film	Roughness R_q [nm]	Average height D [nm]
ZnO	7.93	32.4
ZnO:Cu(1.5 at.%)	6.22	23.4
ZnO:Cu(3.3 at.%)	5.48	21.0
ZnO:Cu(5.0 at.%)	4.90	16.6
ZnO:Ag(1.6 at.%)	24.0	83.5
ZnO:Ag(5.9 at.%)	27.0	120

3.3. Temperature evolution of the absorption edge

Zinc oxide is a wide bandgap semiconductor and therefore is characterized by wide transparency range in visible region. The investigations of the optical properties first of all were concentrated on the investigations of temperature behaviour of the absorption edge in silver and copper doped ZnO films. In Fig. 4 the absorption spectra of ZnO films undoped and doped with Ag and Cu are shown in the vicinity of optical absorption edge ($T = 100$ K). As one can notice, absorption edge becomes more slanted and shifts toward the lower energies due to the influence of dopant. Besides, the ZnO films with highest dopant amount is characterised by the highest absorption in the transparency region of ZnO which can be attributed to influence of the metallic clusters the phases of which were observed in XRD spectra.

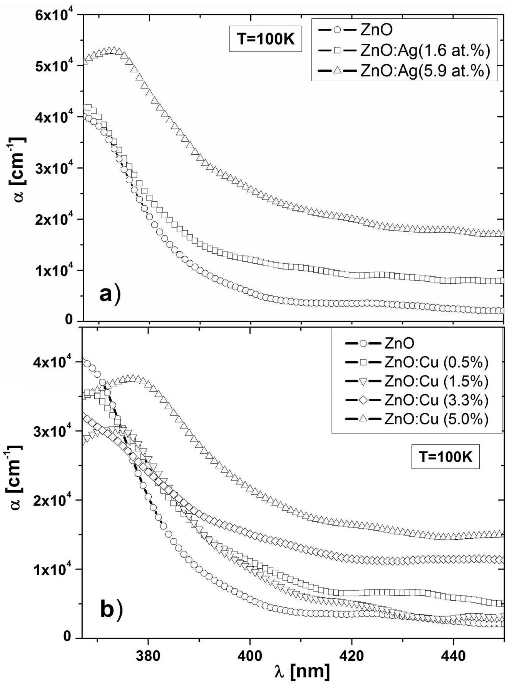

Fig. 4. Optical absorption edge of ZnO:Ag (a) and ZnO:Cu (b) films measured at 100 K.

Temperature behaviour of the absorption edge of ZnO single crystal is described by empirical Urbach's rule. In this case the absorption coefficient can be given as [27, 28]:

$$\alpha(\hbar\omega, T) = \alpha_0 \exp\left(\frac{\sigma}{k_{\mathrm{B}}T}\,(\hbar\omega - E_0)\right), \tag{3}$$

where α_0,E_0 are Urbach's rule parameters which characterize a crystal, k_{B} is the Boltzmann constant, parameter σ defines the slope of the spectral curves.

For all the films (ZnO, ZnO:Ag and ZnO:Cu) in the temperature range 80 ÷ 280 K the dependence $\ln(\alpha) = f(E)$, presented in Fig. 5, has a linear character which confirms the exponential dependence of absorption coefficient on photon energy according to Eq. (3). The slope of these curves remains practically the same and we observe a parallel shift toward lower energy. This provides a basis for assuming that the temperature variation of absorption edge in the studied films is described by a modified Urbach rule [29, 30]:

$$\alpha(\hbar\omega, T) = \alpha_0 \exp\left(\frac{h\nu - E_{\mathrm{g}}(T)}{W}\right), \tag{4}$$

where $W = W_{\mathrm{s}} + W_{\mathrm{d}}$, W_{s} and $W_{\mathrm{d}} = k_{\mathrm{B}}T/\sigma$ characterize static and dynamic disorder due to "frozen" and thermal phonons in the system, respectively. According to this rule, the slope of energy dependence of logarithm of the absorption coefficient in contrast to bulk materials does not change with temperature increase and parallel shift of these dependences into direction of lower energy takes place. Such a behaviour is usual for amorphous or polycrystalline materials [27].

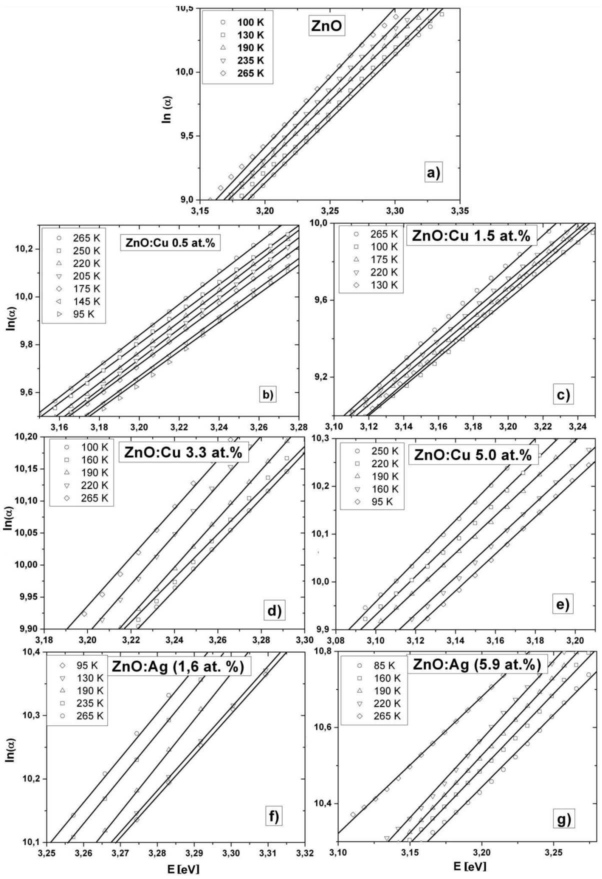

Fig. 5. Dependences $\ln(\alpha) = f(E)$ for the films: (a) ZnO; (b) ZnO:Cu(0.5 at.%); (c) ZnO:Cu(1.5 at.%); (d) ZnO:Cu(3.3 at.%); (e) ZnO:Cu(5.0 at.%); (f) ZnO:Ag(1.6 at.%); (g) ZnO:Ag(5.9 at.%).

In the case when the thermal phonon mechanism predominates in broadening of the absorption edge, the temperature dependence of parameter $\sigma(T)$, describing the slope of the optical absorption edge is following [31]:

$$\sigma(T) = \sigma_0 \frac{2k_{\mathrm{B}}T}{h\nu_{\mathrm{ph}}}\,\mathrm{th}\left(\frac{h\nu_{\mathrm{ph}}}{2k_{\mathrm{B}}T}\right), \tag{5}$$

where σ_0 is constant, which is inverse proportional to the electron– (exciton–) phonon interaction, $h\nu_{\mathrm{ph}}$ is the effective energy of phonons participating in absorption edge formation.

Temperature dependence $\sigma(T)$, defined from the slope of $\ln(\alpha) = f(E)$, is shown in Fig. 6. For all the samples, it has a linear character confirmed by their parallelism. Since the parameter $\sigma(T)$ is connected with the slope of absorption edge one can notice that the absorption edge is most bluff in the undoped ZnO film. The dependence of $\sigma(T)$ on the dopant concentration is not monotonic. At the same time this parameter increases at heating for all studied films.

To determine the phonon energies $h\nu_{\mathrm{ph}}$ and σ_0 constants for the investigated films, it is necessary to expand $\mathrm{th}(h\nu_{\mathrm{ph}}/2k_{\mathrm{B}}T)$ in series and take into account first two

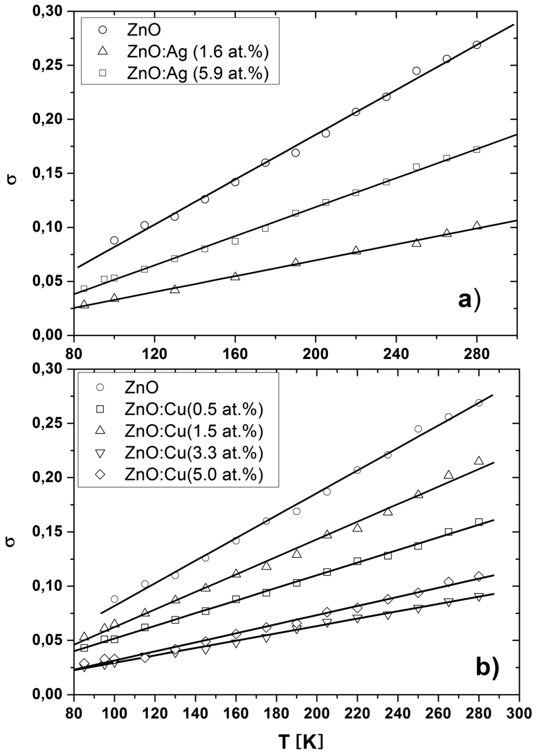

Fig. 6. Temperature dependence of $\sigma(T)$ parameter for the films: (a) ZnO:Ag and (b) ZnO:Cu.

terms [32]:

$$\sigma(T) = \sigma_0 \left[1 - \frac{1}{3}\left(\frac{h\nu_{\text{ph}}}{2k_{\text{B}}T}\right)^2\right]. \tag{6}$$

Drawing the dependence of $\sigma(T)$ from $1/T^2$ and using a linear extrapolation from the side of higher temperatures, the values of ν_{ph} and σ_0 were found for Ag- and Cu-doped ZnO films (Table III). Constant σ_0 is inversely proportional to the strength of electron–(exciton–) phonon interaction g:

$$\sigma_0 = \frac{3}{2}\frac{1}{g}. \tag{7}$$

TABLE III

Obtained values of ν_{ph} and σ_0 for the ZnO, ZnO:Ag and ZnO:Cu films.

Film	σ_0	ν_{ph} [cm^{-1}] ([meV])
ZnO	0.363	347 (43.0)
ZnO:Ag(1.6 at.%)	0.235	349 (43.3)
ZnO:Ag(5.9 at.%)	0.164	418 (51.9)
ZnO:Cu(0.5 at.%)	0.234	383 (47.5)
ZnO:Cu(1.5 at.%)	0.328	397 (49.2)
ZnO:Cu(3.3 at.%)	0.132	375 (46.5)
ZnO:Cu(5.0 at.%)	0.161	384 (47.6)

Therefore, in ZnO films the strength of electron–(exciton–) phonon interaction grows with the dopant (Ag or Cu) amount increasing. The calculated effective energies of phonons can be referred to the transverse optical phonons. Their wave number in the bulk ZnO is 380 cm^{-1} [33].

However, the direct determination of band-gap energy E_{g} is complicated when the Urbach broadening of absorption edge takes place. In this case the isoabsorption dependence $E'(T)$ would reflect the temperature behaviour of E_{g} parameter. The values of E' correspond to a certain fixed absorption $\alpha = \text{const}$ (usually $0.3 < \alpha d < 3$, where d is the thickness of a sample). In Fig. 7 the "isoabsorption" temperature dependence of energy E' ($\alpha = 2 \times 10^4$ cm^{-1}) is shown for the films doped with Ag and Cu. As it is clearly seen, the energy E' decreases at heating. Therefore, one can conclude that the bandgap energy E_{g} also decreases with temperature increase and the situation looks very similar for all the doped films.

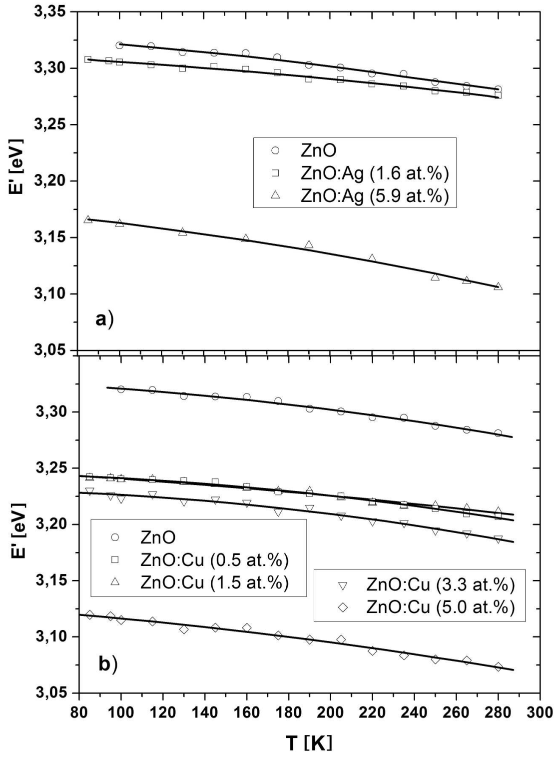

Fig. 7. Temperature dependence of $E'(T)$ in ZnO:Ag (a) and ZnO:Cu (b) films.

Such temperature behaviour of E' is typical for crystalline materials. This confirms that the mechanisms of shifting and broadening of the optical absorption edge are similar for crystalline as well as for the polycrystalline and glassy materials and thermal phonons play a considerable role in these mechanisms. The fulfilment of the modified Urbach rule testifies that the investigated Ag- and Cu-doped ZnO films are polycrystalline with quite small sizes of the crystallites. This conclusion correlates fairly well with the data of AFM analysis.

4. Conclusions

The Ag- and Cu-doped ZnO films prepared by rf-magnetron sputtering on glass substrates are characterized by a wurtzite structure with the c-axis perpendicular to the film surface. The mechanisms of Ag and Cu incorporation into ZnO structure were discussed and the shift of (002)-peak of wurtzite ZnO into direction of higher values of 2θ was found to be connected with the isomorphous substitution of Zn^{2+} ions by Ag^{+} or Cu^{2+} ions. The morphological parameters taken from AFM investigations indicate that the presence of Ag dopant in ZnO involves a larger grain growth together with increasing roughness, whereas the presence of Cu dopant decreases a little the grain sizes. The temperature behaviour of the optical absorption edge in ZnO:Ag and ZnO:Cu films was described by a modified Urbach rule. The strength of electron– (exciton–) phonon interaction together with the energy of phonons was found to grow with a dopant (Ag or Cu) amount increasing in ZnO films. The doping of ZnO with copper or silver permits the purposeful modification of its optical parameters, for example, energy position and shape of optical absorption edge.

References

[1] B.J. Lokhande, M.D. Uplane, *Appl. Surf. Sci.* **167**, 243 (2000).

[2] R. Triboulet, J. Perrière, *Prog. Cryst. Growth Charact. Mater.* **47**, 65 (2003).

[3] E. Fortunato, P. Barquinha, A. Pimentel, L. Pereira, A. Gonçalves, A. Marques, R. Martins, L. Pereira, *Appl. Phys. Lett.* **85**, 2541 (2004).

[4] D. Brida, E. Fortunato, I. Ferreira, H. Aguas, R. Martins, *J. Non-Cryst. Solids* **299-302**, 1272 (2002).

[5] Ü. Özgür, Ya.I. Alivov, C. Liu, A. Teke, M.A. Reshchikov, S. Doğan, V. Avrutin, S.-J. Cho, H. Morkoç, *J. Appl. Phys.* **98**, 1 (2005).

[6] M. Öztas, M. Bedir, *Thin Solid Films* **516**, 1703 (2008).

[7] L. Duan, W. Gao, R. Chen, Z. Fu, *Solid State Commun.* **145**, 479 (2008).

[8] D. Chakraborti, G.R. Trichy, J.T. Prater, J. Narayan, *J. Phys. D, Appl. Phys.* **40**, 7606 (2007).

[9] S.W. Xue, X.T. Zu, W.L. Zhou, H.X. Deng, X. Xiang, L. Zhang, H. Deng, *J. Alloys Comp.* **448**, 21 (2008).

[10] S.H. Jeong, B.N. Park, S.B. Lee, J.-H. Boo, *Surf. Coat. Technol.* **193**, 340 (2005).

[11] T. Kryshtab, V.S. Khomchenko, V.B. Khachatryan, N.N. Roshchina, J.A. Andraca-Adame, O.S. Lytvyn, V.I. Kushnirenko, *J. Mater. Sci. Mater. Electron.* **18**, 1115 (2007).

[12] R. Deng, Y. Zou, H. Tang, *Physica B* **403**, 2004 (2008).

[13] S.T. Kuo, W.H. Tuan, J. Shieh, S.F. Wang, *J. Europ. Ceram. Soc.* **27**, 4521 (2007).

[14] Y. Zhang, L. Wu, H. Li, J. Xu, L. Han, B. Wang, Z. Tuo, E. Xie, *J. Alloys Comp.* **473**, 319 (2009).

[15] P. Singh, A. Kaushal, D. Kaur, *J. Alloys Comp.* **471**, 11 (2009).

[16] T. Ratana, P. Amornpitoksuk, T. Ratana, S. Suwanboon, *J. Alloys Comp.* **470**, 408 (2009).

[17] D.B. Buchholz, R.P.H. Chang, J.H. Song, J.B. Ketterson, *Appl. Phys. Lett.* **87**, 082504 (2005).

[18] H. Gong, J.Q. Hu, J.H. Wang, C.H. Ong, F.R. Zhu, *Sensors Actuators B Chem.* **115**, 247 (2006).

[19] J. Fan, R. Freer, *J. Appl. Phys.* **77**, 4795 (1995).

[20] C.A.K. Gouvea, F. Wypych, S.G. Moraes, N. Duran, P. Peralta-Zamora, *Chemosphere* **40**, 427 (2000).

[21] S.H. Jeong, D.G. Yoo, D.Y. Kim, N.E. Lee, J.H. Boo, *Thin Solid Films* **516**, 6598 (2008).

[22] V.S. Khomchenko, T.G. Kryshtab, A.K. Savin, L.V. Zavyalova, N.N. Roshchina, V.E. Rodionov, O.S. Lytvyn, V.I. Kushnirenko, V.B. Khachatryan, J.A. Andraca-Adame, *Superlatt. Microstruct.* **42**, 94 (2007).

[23] Q. Wan, Z. Xiong, J. Dai, J. Rao, F. Jiang, *Opt. Mater.* **30**, 817 (2008).

[24] X.B. Wang, D.M. Li, F. Zeng, F. Pan, *J. Phys. D, Appl. Phys.* **38**, 4104 (2005).

[25] X. Peng, J. Xu, H. Zang, B. Wang, Z. Wang, *J. Lumin.* **128**, 297 (2008).

[26] A. Tiwari, M. Snure, D. Kumar, J.T. Abiade, *Appl. Phys. Lett.* **92**, 062509 (2008).

[27] B.I. Turko, V.B. Kapustianyk, V.P. Rudyk, G.A. Lubochkova, B.A. Simkiv, *J. Appl. Spectrosc.* **73**, 222 (2006).

[28] S. Ilican, Y. Caglar, M. Caglar, *J. Optoelectron. Adv. Mater.* **10**, 2578 (2008).

[29] J. Tauc, *Mater. Res. Bull.* **5**, 721 (1970).

[30] N.E. Mott, E.A. Davis, *Electronic Processes in Non-Crystalline Materials*, Oxford University Press, London 1982.

[31] I.P. Kuz'mina, A.N. Lobachev, N.S. Triodina, *A Study of Crzstal Synthesis in Hydrothermal Conditions*, Ed. A.N. Lobachev, Nauka, Moscow, 1970, p. 29, (in Russian).

[32] S. Pačesova, B. Bržezina, L. Jastrabik, *Phys. Status Solidi B* **116**, 545 (1985).

[33] B.K. Meyer, H. Alves, D.M. Hofmann, W. Kriegseis, D. Forster, F. Bertram, J. Christen, A. Hoffmann, M. Strabburg, M. Dworzak, U. Haboeck, A.V. Rodina, *Phys. Status Solidi B* **241**, 231 (2004).